

# *Design of a High-Speed Electro-Absorption Modulator Based on Graphene and Microfiber*

Yongqiang Xie<sup>1</sup>, Jiayuan Li<sup>1</sup> and Ke Xu\*

<sup>1</sup> Dept. of Electronic and Information Engineering, Harbin Institute of Technology (Shenzhen), Shenzhen, China, 518055  
[kxu@hit.edu.cn](mailto:kxu@hit.edu.cn)

**Abstract**—A high-speed traveling wave electro-absorption modulator based on graphene-micro fiber is designed. Graphene modulates the optical transmission intensity by changing its fermi level under different applied voltages. Graphene has an extremely high carrier mobility which has a potential electrical bandwidth of 500 GHz. However, the bandwidth of the state-of-art graphene based modulator is limited by the RC constants rather than the carrier transit time. Here we apply the traveling wave electrodes to improve the bandwidth of the graphene-microfiber modulator. The coplanar strip electrodes are designed to match the group velocity of the microwave and optical signal. We also target to reduce the RF loss and realize the impedance matching. We have designed a graphene-microfiber electro-absorption modulator with 15dB extinction ratio and 62GHz electrical bandwidth.

**Keywords**—graphene-micro fiber; electro-absorption; traveling wave electrode; modulator

## I. INTRODUCTION

The electro absorption modulator (EAM) plays an important role in the optical fiber communications due to its advantages of compact structure, low power consumption, intrinsic fast response and so on. The EAM based on Franz-Keldysh effect has been realized on a variety of material system like Ge [1], SiGe [2], GaAs [3], quantum well [4] and etc. More recently, graphene emerges as a promising 2D material that is suitable for electro-absorption modulation due to its linear dispersion relation, tunable fermi level and extremely high carrier mobility [5]. Besides, the atomic thick graphene sheet is easy to be integrated with the photonic integrated circuits or fibers by mature transfer process. Graphene has been considered as an excellent material for electro-absorption modulation and it has been demonstrated on different substrate like optical fiber [6], silicon and silicon nitride [7,8]. Though graphene promises as high as 500 GHz electrical bandwidth, the graphene based modulator is limited by the RC constant of the device itself. For the graphene microfiber modulator, the required modulation length is normally a few millimeters. The group velocity mismatch of the optical wave in fiber and the electrical wave applied to the electrodes have to be considered for high speed modulation.

In this paper, a traveling wave electro-absorption (TW-EAM) is designed for high speed operation. The extinction ratio of the EAM is 15dB and the microwave attenuation is 0.712 dB/mm. The characteristic impedance is calculated to be 54.3 ohm at RF frequency 62 GHz. The electrical-electrical (EE) S21 simulation of the loaded transmission line is performed using the frequency dependent RLGC values obtained from the finite element method (FEM)

based simulations. The electro-absorption (EA) 3dB bandwidth coincides with the electrical 6.4 dB bandwidth at 62 GHz.

## II. DEVICE DESIGN AND ANALYSIS

### A. Light-Graphene Interaction

The graphene-micro fiber (GMF) is designed on a MgF<sub>2</sub> substrate. The schematic diagram of the device is depicted in Fig.1, where a microfiber is placed onto a graphene film, which is transferred on the gap between two Ag electrodes. The refractive index of the MgF<sub>2</sub> substrate is a bit smaller than the microfiber to reduce the light leakage into the substrate. The diameter of the core and cladding of the microfiber are 0.25μm, 3μm, respectively and the evanescent wave interacts with the graphene underneath. A coplanar metal strip is designed for traveling wave electrodes of the device. The electrodes are 7 μm away from the microfiber to ensure negligible loss induced from the metal and this value is also optimized considering the electrode impedance. The graphene's permittivity can be obtained from the Kubo formula [9]. The optical mode in the graphene-microfiber on MgF<sub>2</sub> substrate for our proposed structure was numerically simulated using FEM.

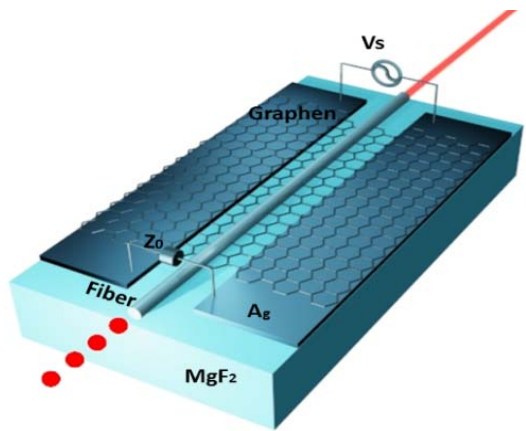


Fig. 1. The schematic diagram of the proposed TW-EAM structure

The graphene's single layer thickness is set to be 0.7nm in the simulations. As shown in Fig. 2, the attenuation of the proposed modulator can be calculated by the imaginary part of the effective index. Transmission loss is calculated to be 2.41dB/cm at 0.7eV (ON state) and 83.22 dB/cm at 0eV (OFF state), respectively. The extinction ratio of the EAM is 15dB by tuning the Fermi level of the graphene from 0eV to 0.7eV with a device length of 1.85mm. The optical group index is simulated to be 1.458 using the equation from under 0.4eV chemical potentials.

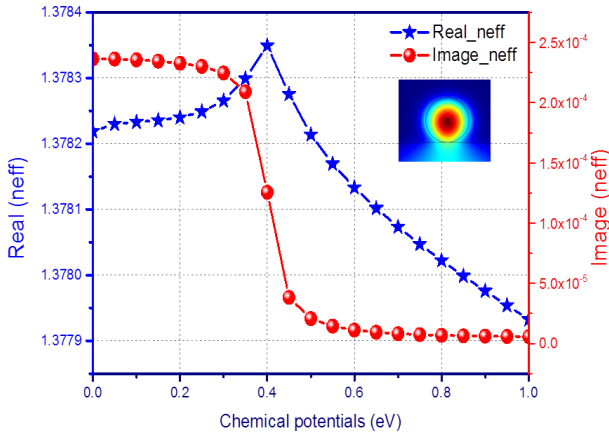


Fig. 2. Real (blue) and imaginary (red) part of effective mode index under different graphene's chemical potentials. Inset: The optical field profile.

### B. Traveling Wave Electrodes Design

The RC limit is the major limiting factor of the modulation speed for the graphene based modulator. Here we show a detail design process for the coplanar strip (CPS) traveling wave electrode using a 3-D full-wave electromagnetic solver to obtain EE S21 response. There are three requirements in the design of the TWE: a) the low microwave attenuation; b) group index matching between the microwave and optical wave; c) the impedance matching between the transmission line and the termination [10].

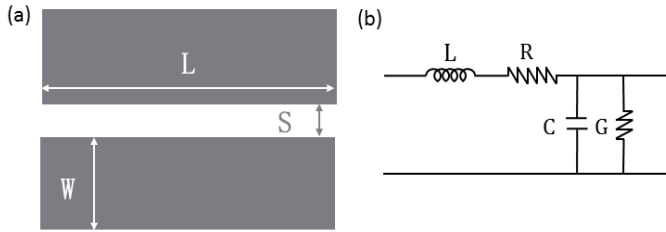


Fig.3.(a) Top-view schematic of the unloaded CPS. (b) Simplified equivalent circuit model of unloaded transmission line.

Fig.3 (a) shows the schematic diagram of the electrode structure and the corresponding equivalent circuit model. The structural parameters of the electrode are optimized by the following process. We first simulate the s-parameters using the FEM 3D full-wave electromagnetic solver. The s-parameters are converted to ABCD parameters using the method that was previously summarized in [11]. Then, the attenuation, effective index n, and characteristic impedance Z are obtained from the ABCD parameters and are plotted in Fig. 4. It can be seen that the characteristic impedance Z and microwave effective index do not change too much at high frequency regime while the microwave loss increases at high frequencies. The structural parameters are determined by considering the requirements of RF and optical wave group velocity matching, impedance matching and low RF loss. Under these considerations, we have obtained a set of structural parameters of the electrode: electrode width: W=168  $\mu\text{m}$ ; electrode spacing: S=17.2  $\mu\text{m}$ ; electrode length: L =1.86 mm; electrode thickness: H=2  $\mu\text{m}$ . The corresponding

microwave attenuation is 0.712dB/mm, the RF effective index is 1.58 and the characteristic impedance is 54.3 ohm which is matched with the 50 ohm system.

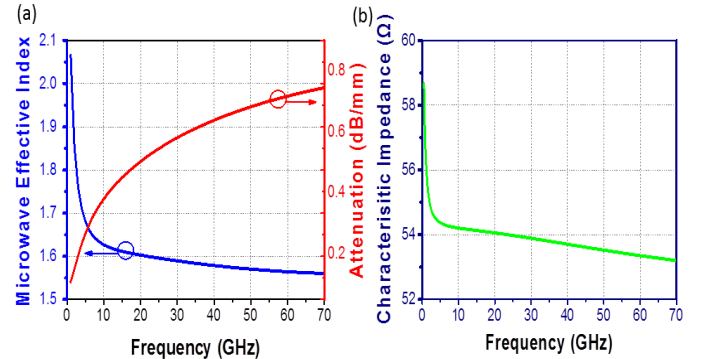


Fig.4 Simulated (a), microwave index (blue), microwave attenuation (red), and (b) characteristic impedance of CPS transmission lines.

Then, we use the RLGC of CPS transmission line circuit model in Fig.3 (b) to calculate the electrical frequency response. This model applies under the assumption of transverse electro-magnetic or quasi-TEM wave propagation [12]. The RLGC can be calculated from equation (1) (2) and (3), and they are plotted in Fig. 5.

$$Z = \sqrt{\frac{R+j\omega L}{G+j\omega C}} \quad (1)$$

$$\gamma = \alpha + j\beta = \frac{1}{2}(\frac{R+GZ}{Z} + j\omega\sqrt{LC}) \quad (2)$$

$$n = \frac{c_0}{v} = c_0\sqrt{LC} = c_0ZC = c_0\frac{L}{C} \quad (3)$$

where,  $\gamma$  is propagation constant,  $\beta$  is the microwave velocity,  $\beta=\omega/v$ .

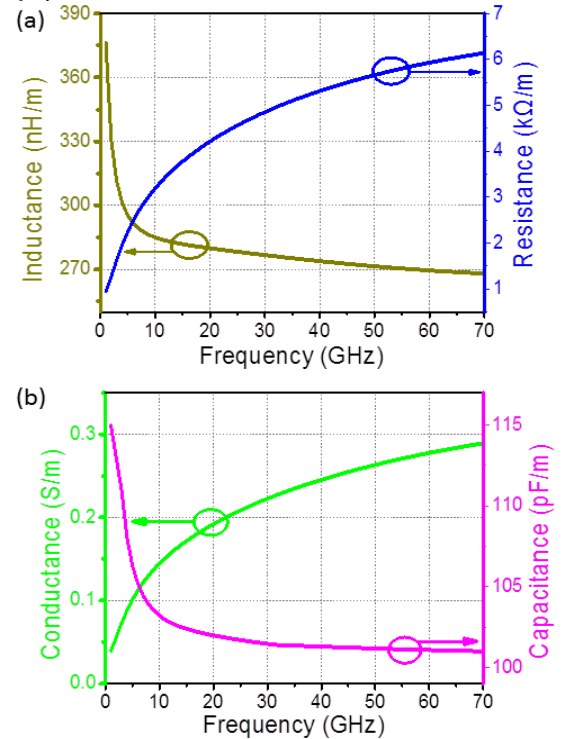


Fig.5. Simulated (a) resistance (blue); inductance (gray); (b) conductance (green); capacitance (pink) per unit length of the CPS transmission lines.

We then calculate the electrical-electrical (EE) S21 response of the loaded transmission line using the frequency

dependent RLGC values obtained from the FEM simulations which is plotted as the blue curve in Fig. 6. The TW-EAM frequency response is also simulated with the normalization of the RF link gain [13] which is plotted as the red curve in Fig. 6. It can be seen that the electro-absorption (EA) 3dB bandwidth coincides with the electrical 6.4 dB bandwidth at 62 GHz.

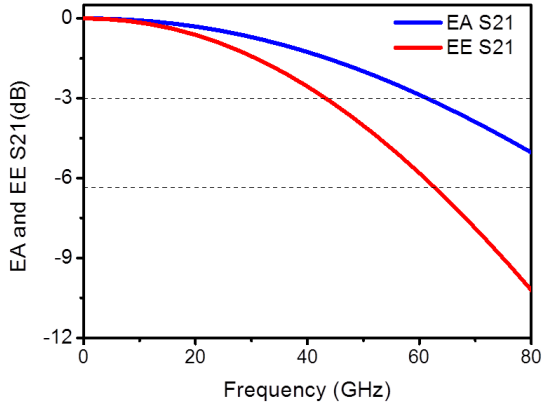


Fig.6 The simulated EE S21 and EA S21 response (the dashed lines correspond to 3dB and 6.4dB, respectively).

### III. CONCLUSION

We have designed a high-speed electro-absorption modulator that based on this 1.85 mm long graphene microfiber structure, tuning the Fermi level of the grapheme from 0eV to 0.7eV achieves 15dB extinction ratio. The electrodes are optimized by matching the optical and electrical group velocity, minimizing the RF attenuation and satisfying the impedance matching. Up to 62 GHz operation bandwidth is achieved using traveling wave electrode.

### ACKNOWLEDGMENT

This work is supported by National Natural Science Foundation of China (NSFC) (61505039) and Shenzhen Municipal Science and Technology Plan Project (JCYJ20150403161923530).

### REFERENCES

- [1] N. Feng, D. Feng, S. Liao, X. Wang, P. Dong, H. Liang, C. Kung, W. Qian, J. Fong, R. Shafiiha, Y. Luo, J. Cunningham, A. Krishnamoorthy, and M. Asghari, "30 GHz Ge electro-absorption modulator integrated

- with 3 $\mu$ m silicon-on-insulator waveguide," Optics Express, vol. 19, no. 8, pp. 7062-7067, September 2011.
- [2] D. Feng, W. Qian, H. Liang, C. Kung, Z. Zhou, Z. Li, J. Levy, R. Shafiiha, J. Fong, B. Luff, and M. Asghari, "High-Speed GeSi Electroabsorption Modulator on the SOI Waveguide Platform," IEEE Journal of Selected Topics in Quantum Electronics, vol. 19, vo. 6, pp. 64-73, Novermber 2013.
- [3] S. Lee, C. Park, J. You, H. Yoon, Y. Cho, and Y. Park, "850 nm IR transmissive electro-absorption modulator using GaAs micromachining," Sensors and Actuators A: Physical, vol.197, no 1, pp. 47-52, August 2013.
- [4] P. Chaisakul, D. Marrismorini, M. Rouifed, G. Isella, D. Chrastina, J. Frigerio, X. Roux, S. Edmond, J. Coudeville, and L. Vivien, "23 GHz Ge/SiGe multiple quantum well electro-absorption modulator," Optics Express, vol. 3, no. 1, pp. 86-95, 2011.
- [5] X. Jia, J. Camposdelgado, M. Terrones, V. Meuniernd, and M. Dresselhaus, "Graphene edges: a review of their fabrication and characterization," Nanoscale, vol. 3, no. 1, pp. 86-95, November 2013.
- [6] F. Zhou, X. Jin, R. Hao, X. Zhang, H. Chi, and S. Zheng, "A graphene-based all-fiber electro-absorption modulator," Journal of Optics, Vol. 45, pp. 337-342, May 2016.
- [7] M. Liu, X. Yin, E. Ulinavila, B. Geng, T. Zentgraf, L. Ju, F. Wang and X. Zhang, "A graphene-based broadband optical modulator," Nature, vol. 474, no. 7349, pp. 64-67, June 2011.
- [8] L A. Shiramin, D. Van Thourhout, "Graphene Modulators and Switches Integrated on Silicon and Silicon Nitride Waveguide," IEEE Journal of Selected Topics in Quantum Electronics, vol. 23, no. 1, pp. 1-7, June 2016.
- [9] L. Yang, T. Hu, R. Hao, C. Qiu, C. Xu, H. Yu, Y. Xu, X. Jiang, Y. Li and J. Yang, "Low-chirp high-extinction-ratio modulator based on graphene-silicon waveguide," Optics Letters, vol. 38, no. 14, pp. 2512-2515, July 2013.
- [10] Z. Han, S. Tang, D. An, L. Sun, X. Lu, Z. Shi, Q. Zhou and R.Chen, "High-Speed Traveling-wave Electrodes for Polymeric Electro-Optic Modulators," Part of the SPIE Conference on Optoelectronic Interconnects VI, vol. 3632, pp. 354-362, April 1999.
- [11] X. Liu, Z. Zhu, Y.Yan, F. Wang, and R. Ding, "Reduction of signal reflection along through silicon via channel in high-speed three-dimensional integration circuit," Chinese Physics B, vol. 23, no. 3, January 2014.
- [12] D. Patel, S. Ghosh, M. Chagnon, A. Samani, Venkat Veerasubramanian, M. Osman, and D.V. Plant, "Design, analysis, and transmission system performance of a 41 GHz silicon photonic modulator," Optics Express, vol. 23, no. 11, pp. 14263-14287, June 2015.
- [13] G L. Li, C K. Sun, S A. Pappert, W X. Chen, and P K. Yu, "Ultrahigh-speed traveling-wave electroabsorption modulator-design and analysis," IEEE Transactions on Microwave Theory and Techniques, vol. 47, no. 7, pp. 1177-1183, 1999